Int. J. Cancer: **124,** 2755–2765 (2009)

FAST TRACK

Polyproline-type helical-structured low-molecular weight heparin (LMWH)-taurocholate conjugate as a new angiogenesis inhibitor

Esak Lee[1], Yoo-Shin Kim[2], Sang Mun Bae[2], Sang Kyoon Kim[1], Shunji Jin[1], Seung Woo Chung[1], Myungjin Lee[3], Hyun Tae Moon[4], Ok-Cheol Jeon[4], Rang Woon Park[2], In San Kim[2], Youngro Byun[1]* and Sang Yoon Kim[3]*

[1]*College of Pharmacy, Seoul National University, Seoul 151-742, South Korea*
[2]*Department of Biochemistry and Cell Biology, School of Medicine, Kyungpook National University, Jung-Gu, Daegu 700-422, Republic of Korea*
[3]*Department of Otolaryngology-Head and Neck Surgery, Asan Medical Center, College of Medicine, University of Ulsan, Seoul 138-736, South Korea*
[4]*Mediplex Corp. Korea, Seoul 152-711, South Korea*

Although heparin can regulate angiogenesis, tumor growth and metastasis, its clinical application, as well as that of low-molecular heparin (LMWH), for treating cancer are limited because of heparin's anticoagulant activity and risk of hemorrhages. LMWH-taurocholate conjugates (LHT7), which have low anticoagulant activity, were synthesized. The structural property of LHT was evaluated by circular dichroism and the binding affinity of LHT7 to vascular endothelial growth factor 165 ($VEGF_{165}$) was measured by isothermal titration calorimetry. The inhibitory effect of LHT7 on VEGF-mediated KDR (VEGF-receptor 2) phosphorylation in Human umbilical vein endothelial cells was evaluated. The $VEGF_{165}$ dependent Matrigel plug assay was performed to verify the antiangiogenic potential of LHT7 on a $VEGF_{165}$ inhibitor. Finally, tumor growth inhibition effects of LHT7 on SCC7 and the survival rate of animal models were investigated. Moreover, MDA-MB231 xenograft mouse model was additionally used to confirm the therapeutic effect of LHT7 on human breast cancer cell line. As a result, LHT7 which has 12.7% of anticoagulant activity of the original LMWH showed a peculiar polyproline-type helical structure. LHT7 binds to VEGF strongly and inhibits VEGF dependent KDR phosphorylation. The results of Matrigel plug assay proved LHT7 as a strong antiangiogenic agent inhibiting $VEGF_{165}$. Remarkably, LHT7 showed a significant tumor growth inhibition potential on SCC7 with an increased survival rate. LHT7 also delayed tumor growth in MDA-MB231 human breast cancer cell lines.

Key words: LMWH-taurocholate conjugate; angiogenesis; polyproline-type helical structure; vascular endothelial growth factors 165 ($VEGF_{165}$)

Angiogenesis, the formation of new blood vessels from existing vasculature, is a fundamental process for tumor growth, metastasis and other angiogenic diseases.[1] Recently, angiogenesis has been established as a crucial target for cancer treatment, as the process of new blood vessel formation is required to supply oxygen and nutrients needed for tumor growth when a cancer cell reaches a certain size.[2,3] Moreover, angiogenic microvascular endothelial cells became a cardinal target for therapeutic intervention since they are easily accessible.[4,5]

Angiogenesis is a multistep process that involves endothelial cell activation, proliferation, migration, the proteolytic degradation of the extracellular matrix and the formation of capillary vessels. To trigger this process, tumor cells release a number of angiogenic growth factors such as vascular endothelial growth factor (VEGF), fibroblast growth factor basic (bFGF) and scatter factors.[6–8] Many angiogenic proteins, which are potential targets for pharmacological inhibitory strategies, depend on heparan sulfate for their biological functions.[9,10] Heparan sulfate is found on the cell surface and in the extracellular matrix where it plays a central role in growth factor regulation. It has been reported that bFGF and several isoforms of VEGF depend on the mechanics of prototypic heparan sulfate.[11–14] For this reason, heparin, which has structural similarities with heparan sulfate, has been highlighted as a growth factor inhibitory therapeutic agent beyond its anticoagulant indications.

Heparin is a highly sulfated glycosaminoglycan (GAG) and a potent inhibitor of blood coagulation, which is mainly attained through the formation of complex with antithrombin III.[15–17] Moreover, heparin can affect angiogenesis on the basis of binding with angiogenic growth factors.[18] The interaction between heparin and growth factors is mediated by the physiochemical properties of heparin, which are bestowed by its sulfation pattern, charge distribution, overall charge density and molecular size.[13] Nevertheless, heparin-based therapeutic approaches are limited, because the therapeutic effects of heparin are not strong enough to apply to clinical uses. Apart from the lack of its strong therapeutic effect, it is also noted that it causes the side effect of hemorrhage.

Several chemically modified heparin derivatives such as heparin-steroid conjugates, heparin-polystyrene derivatives, bile acid-acylated heparin derivatives and neoheparin have been synthesized to overcome these clinical limitations.[19–23] Those chemically modified heparin conjugates have an advantage in decreasing the risk of bleeding, as well as enhancing other biological activities of heparin, which prevents angiogenesis, metastasis and cell proliferations. In particular, bile acid-acylated heparin derivatives showed higher anticancer effects than heparin alone due to their carrier effect based on EPR effects, antiangiogenic activities and cell internalized apoptotic effects.[20–22]

On the basis of previous studies about bile acid-acylated heparin derivatives, new low-molecular heparin (LMWH)-taurocholate derivatives (LHT) were prepared to make covalent bonding between the amine group of *N*-taurocholylethylenediamine (TCA-NH_2) and carboxylic acids in the LMWH *via* amide formations. The LHT derivatives, we have developed for this study have, an academic novelty since these conjugates have quite different prop-

Esak Lee and Yoo-Shin Kim contributed equally to this work as first authors.

Youngro Byun and Sang Yoon Kim contributed equally to this work as corresponding authors.

Grant sponsor: Next Generation New Technology Development Program [Korea Ministry of Commerce, Industry, and Energy (MOCIE)]; Grant number: 10011353.

***Correspondence to:** College of Pharmacy, Seoul National University, 599 Gwanak-ro, Sillim-9-dong, Gwanak-gu, Seoul 151-742, South Korea. Fax: +82-2-872-7864. E-mail: yrbyun@snu.ac.kr or Department of Otolaryngology, Asan Medical Center, College of Medicine, University of Ulsan, Seoul 138-736, South Korea. Fax: +82-2-489-2773. E-mail: sykim2@amc.seoul.kr

Received 8 October 2008; Accepted after revision 5 December 2008
DOI 10.1002/ijc.24239
Published online 23 December 2008 in Wiley InterScience (www.interscience.wiley.com).

erties compared with other previous heparin derivatives. LHT can have a diverse range of anticoagulant activities as well as highly sulfated patterns; hence, we can evaluate the relationship between anticancer effects, anticoagulant activities and its sulfation pattern. Thus, the optimal condition of heparin derivatives in anticancer therapy was proposed.

We systematically evaluated the therapeutic potential of LHT as an effective anticancer agent by focusing on its antiangiogenic behavior using $VEGF_{165}$ dependent *in vivo* Matrigel plug assay, binding assay between LHT and VEGF and Human umbilical vein endothelial cells (HUVECs) phosphorylation assay with or without drugs. To evaluate therapeutic potentials of LHT in solid tumors, tumor inhibitory experiments were performed using SCC7 cancer cell. LHT2, LHT7 and LMWH were administered once per 3 days to be compared with the control group. To observe the effect of dosage and injection intervals of LHT7, we varied the drug dosage (0.5, 1 and 5 mg/kg) and the administration schedule (once/day, 2 days, 3 days and 7 days). Finally, cancer disease models which were grafted with MDA-MB231 human breast carcinoma were used in tumor inhibition test to evaluate the therapeutic validity of LHT7 (1, 5 mg/kg/day) on the human cancer cell lines.

Material and methods

Materials

Low-molecular-weight-heparin (LMWH, Fraxiparin®; average MW 4.5 kDa) was purchased from GlaxoSmithKline (Brentford, UK). Taurocholic acid sodium salt (TCA), 1-ethyl-3-(3-dimethylaminopropyl)carbodiimidehydrochloride (EDAC), 4-nitrophenyl chloroformate (4-NPC), triethylamine, *N*-hydroxysuccinimide (HOSu), 4-methylmorpholine, 1,4-dioxane, 2% ninhydrin reagent and trypsin-EDTA were obtained from Sigma Chemical Co. (St. Louis, MO). *N*,*N*-dimethylformamide (DMF), ethylene diamine, formamide and acetone were purchased from Merck (Darmstadt, Germany), and Coatest Factor Xa assay kits were from Chromogenix (Milano, Italy). The Matrigel was obtained from BD bioscience (San Jose, CA), and vascular endothelial growth factor 165 ($VEGF_{165}$) was purchased from Peprotech (Rocky Hill, NJ).

Preparation of LMWH-taurocholate conjugate

Taurocholic acid sodium salt (0.50 g) was mixed with DMF (4.6 ml) and the mixture was agitated at 0°C (Fig. 1). Then triethylamine (0.565 g) and 4-NPC (0.937 g) were added to the taurocholate (TCA) solution, following which, the mixture was reacted for 1 hr at 0°C and 6 hr at room temperature. The reaction solution was centrifuged and filtered. The filtrate was extracted three times from the mixture of ethyl acetate and distilled water. The separated aqueous layer was condensed in vacuum and lyophilized. We could obtain TCA-NPC through these processes with the feed molar ratio of TCA, 4-NPC and triethylamine as 1:5:6. TCA-NPC (0.5 g) was dissolved in 5 ml of DMF solvent and 0.144 g of 4-methyl-morphorline was added, agitating for 1 hr at 50°C. This mixed reactant was dissolved in excess ethylenediamine solution very slowly and we sustained this reaction for 16 hr at room temperature. The feed mole ratio of CB-TCA, 4-methylmorpholine and ethylenediamine was 1:2:100. The product, TCA-NH_2, is water soluble, but ethylenediamine, 4-methylmorpholine and 4-NPC are not dissolved in water. So, the product was recrystallized in acetone to obtain pure TCA-NH_2. After purification, precipitated products were dried under vacuum condition. LMWH was dissolved in distilled water with gentle heat and 0.1 M of HCl was added to maintain the pH condition in the range of 5.5–6.0. To establish several kinds of LMWH-taurocholate derivatives, the feed molar ratio of each reagent was controlled. EDAC was added to the prepared solution and agitated for 5 min to activate carboxylic acid group of LMWH. After that, HOSu was added and agitated for 30 min, followed by slow adding of TCA-NH_2 solution. This reaction was carried out at room temperature and the reaction condition was thoroughly sustained. Unreacted EDAC, HOSu and TCA-NH_2 were removed by dialysis using a membrane of MWCO 2,000 Da.

Characterizations

Several synthesized materials in each step were analyzed using Avance 500 FT-NMR (Bruker, MA), FTIR 4200 spectrometer (Jasco, Japan) and HPLC-1200 series (Agilent technologies, CA). The coupling ratio, defined as the number of taurocholic acid molecules per one heparin molecule, was determined using the UV method.[24–26] The taurocholic acid content in the heparin molecule was detected by the sulfuric acid method, which was developed for the characterization of polysaccharides modified with bile acids.[25] Briefly, an accurately weighed amount of modified heparin was dissolved in water, and an 140 μl of this solution was mixed with 360 μl of pure sulfuric acid at 70°C for 30 min. The final solution was cooled to room temperature and the absorbance was measured at 420 nm against a blank containing the same components as the sample. The anticoagulant activity of LHT was measured by using Coatest Heparin FXa assays kit (Chromogenix, Italy). Circular dichroism spectra of each LHT were measured on a Jasco J-715 circular dichroism detector (Jasco, Japan) over the range of 190–260 nm in PBS using a quartz cuvette with a path length of 0.1 cm. Spectra measurements, taken 6 times with a response rate of 50 nm/min and a data point resolution of 0.5 nm, were averaged to obtain a smooth graph from the data. To check the conformational change of LHT, the circular dichroism of several LHT was recorded under the same condition.

Isothermal titration calorimetry

Isothermal titration calorimetry was performed using a MicroCal VP-ITC titration microcalorimeter (Northampton, MA) at 30°C. $VEGF_{165}$ at a concentration of 17.45 μM in PBS (pH 7.0) was placed in the 1.4 ml calorimeter cell, and LMWH or LHT at a concentration of 350 μM in PBS (pH 7.0) was added sequentially in 6 μl aliquots (for a total of 29 injection) at 5 min intervals. The heat of reaction per injection (microcalories per second) was determined by integration of the peak areas using the Origin Version 5.0 software. This software provides best-fit value of the dissociation constant (K_d) from the plots of the heat evolved per mol of heparin injection *versus* the $VEGF_{165}$/LMWH or LHT molar ratio.

$VEGF_{165}$-mediated KDR phosphorylation assay

HUVECs (HUVECs; Clonetics, San Diego, CA) were cultured at 37°C in 5% CO_2 in Endothelial Cell Basal Medium-2 (EBM-2; Clonetics) supplemented with endothelial growth medium (EGM-2; Clonetics). The cells were incubated in serum-free medium without other supplements for 9 hr and then treated with indicated drugs such as 500 ng/ml of LHT7 and bevacizumab (Avastin®, Roche Pharma) for 1 hr. $VEGF_{165}$ (50 ng/ml) (Peprotech, Rocky Hill, NJ) was preincubated at 37°C for 2 hr and then $VEGF_{165}$ was treated into the cells for 5 min. The treatment was terminated by removal of the medium and washed with cold phosphate-buffered saline with 0.2 mM Na_3VO_4. Cells were solubilized in sample buffer (62.5 mM Tris-HCl, pH 6.8, 2% SDS, 10% glycerol, 50 mM DTT, 0.01% bromophenol blue) and harvested by scraping. Insoluble material was removed by centrifugation at 4°C for 10 min at 14,000*g* and boiled in 100°C for 10 min. The cell lysate was separated by SDS-PAGE and transferred to nitrocellulose membranes. Membranes were probed with rabbit polyclonal anti-phospho-VEGFR2 antibody (Cell Signaling Technology, Beverly, MA) followed by a goat anti-rabbit IgG horseradish peroxidase-conjugated secondary antibody; immunoreactive proteins were detected and visualized by chemiluminescence (ECL kit; Pierce, Rockford, IL).

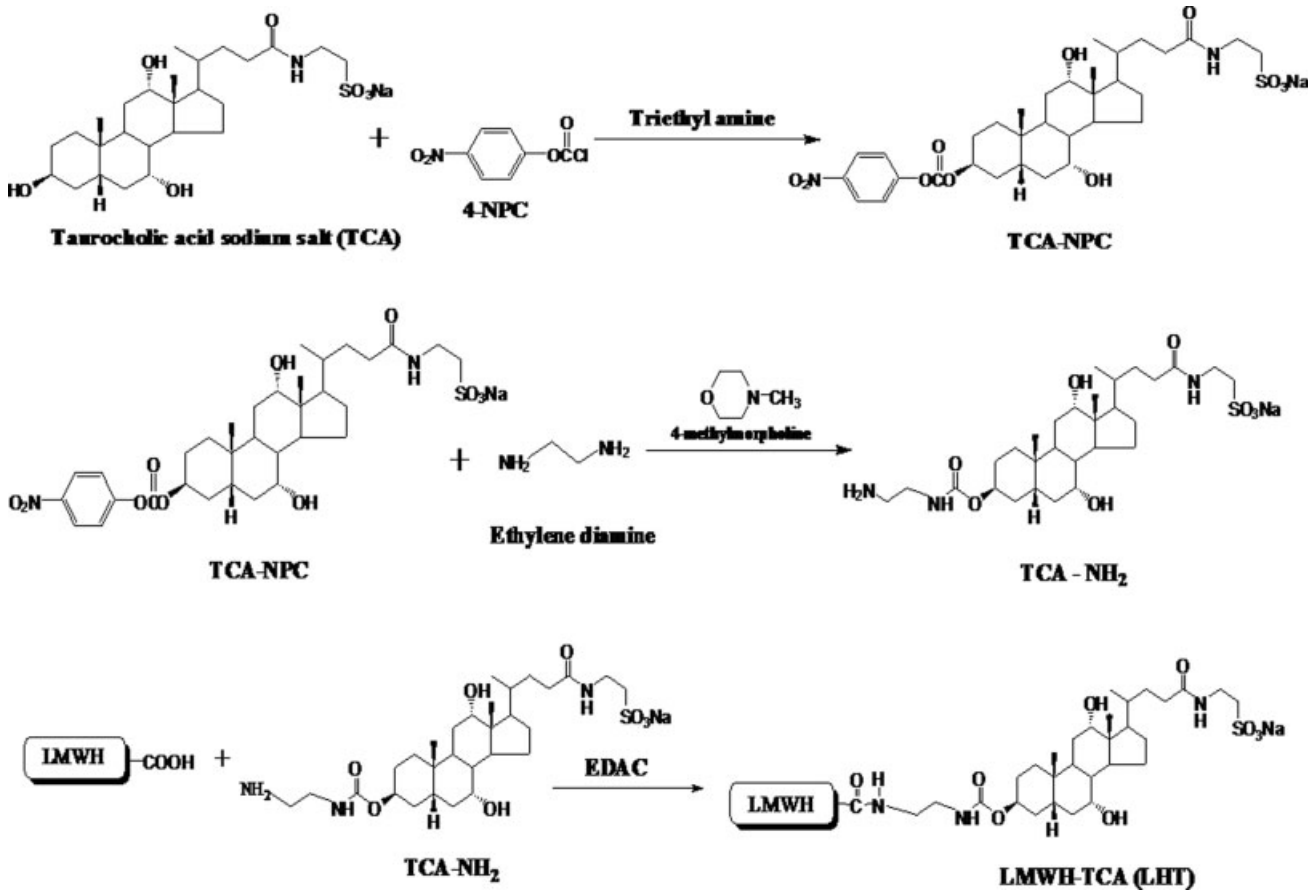

FIGURE 1 – Synthetic scheme for the preparation of LHT. Taurocholic acid sodium salt (TCA) was bound with 4-NPC, forming TCA-NPC urethane bond. TCA-NPC was reacted with a primary amine group of ethylenediamine with a catalytic 4-methyl-morphorline. We put TCA-NPC into the excessive ethylenediamine solution very slowly to prevent a formation of TCA dimers. LHT derivatives were prepared, causing covalent bond between the amine group of *N*- and the carboxylic acids of heparin *via* amide formation.

In vivo *Matrigel plug assay*

These assays were performed as described previously.[21] Briefly, 637 μl of liquid Matrigel-PBS mixture was injected subcutaneously into the flanks of C3H/HeN mice. The Matrigel (BD bioscience, CA) contained $VEGF_{165}$ (Peprotech, Rocky Hill, NJ) at a final concentration of 500 ng/ml to stimulate angiogenesis and heparin or LHT at a final concentration of 500 μg/ml. All treatment groups contained 6 mice and the care and maintenance of animals were undertaken in conformation with the Institutional guidelines of the Institutional Animal Care and Use Committee (IACUC) of our university. After 10 days, mice were sacrificed and Matrigel plugs were removed and fixed in 4% paraformaldehyde. To evaluate angiogenesis, plugs were sectioned with 5-μm thickness and were stained with hematoxylin and eosin (H&E) to observe blood vessels within Matrigel. Microvessel was also assessed by anti-von Willebrand factor (anti-vWF) immunostain on immobilized sections of Matrigel. After rinsing and blocking, the sections were incubated with a rabbit anti-mouse vWF monoclonal antibody (Pharmingen, San Diego, CA) at 1:800 dilution. Furthermore, the hemoglobin (Hb) content within the Matrigel plugs was determined by using the Drabkin's reagent kit (Sigma, St. Louis, MO). The Matrigel plugs were removed and homogenized in hypotonic lysis buffer (250 μl of 0.1% Brij-35 per plug) and centrifuged for 5 min at 5000*g* to measure hemoglobin contents in new blood vessels in the Matrigel plugs. The supernatant was incubated in 0.5 ml of Drabkin's solution for 15 min at room temperature; and the absorbance was measured at 540 nm with Drabkin's solution as a blank. Since absorbance is proportional to the total hemoglobin content, the relative hemoglobin content was calculated *versus* the negative and positive controls.

Inhibition effect of LHT on tumor growth

Male C3H/HeN mice (7-weeks old, Orient Bio, Korea) weighing 24–25 g were given dorsal subcutaneous injection of 1.0×10^6 SCC7 cells. SCC7 cells were originally obtained from the American Type Culture Collection (Rockville, MD) and cultured in the Rosewell Park Memorial Institute medium (RPMI1640 from Sigma Aldrich) containing 10% fetal bovine serum and 1% penicillin-streptomycin. On day 7, when each tumor became palpable, volumes reached 50–70 mm^3 and drug administration was started. In the first experiment, we used 3 kinds of drugs, LMWH, LHT2 and LHT7, with the same dosage of 5 mg/kg and the fixed interval of once per 3 days to evaluate the therapeutic effect of LHT, which have different anticoagulant activities. Next, we selected LHT7 as a target drug, and On the basis of the results of the first experiment, we varied its dosages as 0.5, 1 and 5 mg/kg, respectively, with daily intravenous administration. Then, we fixed the dosage of LHT7 at 1mg/kg and varied its interval of administration as daily, once every other day, once every 3 days and once a week. The mice were given intravenous injections of 100 μl of saline containing each drug for 15 days. Every treatment group contained 8–9 mice. The survival rate in mice which were treated with saline, LMWH (5 mg/kg/2 days) and LHT7 (1 mg/kg/2 days) was evaluated for 2 months.

TABLE I – FEED MOLAR RATIO AND CHARACTERIZATION OF LHT DERIVATIVES

Sample	Feed molar ratio[1]	Coupling ratio[2]	Anticoagulant activity (FXa, %)
LHT1	1:1.2:1.2:1.3	0.9 ± 0.1	90.5
LHT2	1:2.4:2.4:2.6	2.3 ± 0.3	80.7
LHT3	1:3.6:3.6:4	3.0 ± 0.1	31.2
LHT4	1:6:6:6.7	3.6 ± 0.2	17.8
LHT7	1:12:12:13.3	7.2 ± 0.2	12.7

[1]Reaction ratio of LMWH:EDAC:HOSu:TCA-NH_2.–[2]The number of coupled TCA in a LMWH.

To investigate therapeutic potential of LHT7 on human cancer cell line, athymic nude mice (7-weeks old, Institute of Medical Science, Tokyo, Japan) were used for animal experiments. A subcutaneous tumor was established by inoculating 1.0×10^7 MDA-MB231 human breast cancer cells into the back of a mouse. When tumors grew to ~300 mm^3, LHT7 was injected *via* tail vein. Mice were divided into 5 groups and received different injections as follows: (*i*) normal saline (the control group, intravenous injection); (*ii*) LHT7 at 1 mg/kg, 5 mg/kg (intravenous injection). Each sample was injected once everyday for 2 weeks. The care and maintenance of animals were undertaken in conformation with the institutional guidelines of the Institutional Animal Care and Use Committee (IACUC) of our university. The body weights of mice were recorded, and tumor volumes were calculated as $a \times b^2/2$, where a is the largest and b the smallest diameter. After sacrifice, tumor tissues were histologically evaluated using 4, 6-diamidino-2-phenylindole (DAPI), CD34 and Ki67 immunohistochemistry to indicate blood vessel formation and cell proliferation. The number of CD34 positive erythrocyte-filled blood vessels and Ki67 positive proliferating cells were counted and averaged using the 5–6 high-power fields (200×) microscopy.

Statistics

Data are expressed as means ± standard errors (s.e.). The non-parametric *t*-test was used to compare groups, where p values of <0.05 were considered significant.

Results

Characteristics

In the synthesis of LHT, the amine group of *N*-taurocholylethylenediamine was coupled with carboxylic groups of LMWH in the presence of EDAC. The synthetic fidelity was confirmed by the ^{1}H NMR and HPLC. In the ^{1}H NMR spectrum, the amide peak at 8 ppm indicated the presence of amide bonds in all kinds of LHT and the peaks in the range of 0.65–2.1 ppm meant the successful introduction of taurocholate (TCA) moieties. At each step, HPLC analysis was conducted and pure synthetic products were obtained according to their own retention times. We varied feed molar ratio of reactants to obtain several LHT of different anticoagulant activities and measured their coupling ratios. The coupling ratio which represents the amount of coupled TCAs in LHT was calculated by the sulfuric acid method. The coupling ratio of LHT ranged from 1 to 7, and LHT7, which has an entirely saturated form, has a coupling ratio of about 7. The anticoagulant activity of each LHT was measured by using FXa chromogenic assay. The anticoagulant activity decreased with the increasing number of TCA moieties and it varied from 10 to 90%. The characterization of LHT and the feed molar ratios of each reactant were shown (Table I).

Structure study of LHT

Circular dichroism (CD) experiment was conducted for the purpose of structural understanding of LHT. The secondary structures of LHT were investigated and compared among different coupling ratios and anticoagulant activities (Fig. 2*a*). In the cases of LHT1, LHT2 and LHT3, their CD diagrams were so similar with that of LMWH (positive molar ellipticity at the wavelength 200–190 nm and negative value at 220–210 nm) that we could find out the conjugation of TCAs on the LMWH and it did not cause any severe structural changes in the range of 3 TCA moieties. However, LHT4, which has about 3.6 ± 0.2 TCAs per LMWH statistically, abruptly showed a quite different secondary structure (positive molar ellipticity at the wavelength around 210 nm and negative value at 200–195 nm); the conjugation of TCAs was continued to evaluate additional structural changes until the saturation point of heparin active sites was reached. LHT7 was the finalized product whose entire carboxylic acid groups were fully saturated by TCAs, showing a poly-proline helical structure (weak and broad positive molar ellipticity at the wavelength around 230–210 nm and strong, sharp negative value at 210–200 nm), as shown in Figure 2*b*.[27,28]

Binding affinity between LHT7 and VEGF$_{165}$

A representative calorimetric titration at pH 7.0 of the $VEGF_{165}$ with LMWH or LHT7 is shown. Each peak in the binding isotherm (Fig. 3*a*) represents a single injection of LMWH or LHT7. The negative deflections from the baseline in addition of LMWH or LHT7 indicate that heat was evolved (an exothermic process). The enthalpy change associated with each injection of LMWH or LHT7 was plotted *versus* $VEGF_{165}$/LMWH or LHT7 molar ratio. In the binding of LHT7 to $VEGF_{165}$, the K_d value was $(3.21 \pm 0.04) \times 10^{-7}$ M, which represents 60 times stronger binding affinity compared with the case of LMWH binding to $VEGF_{165}$. (The K_d value was $(1.86 \pm 0.10) \times 10^{-5}$ M in the LMWH binding to $VEGF_{165}$) (Fig. 3*a*). The binding affinity of LHT7 to $VEGF_{165}$ is strong enough to be compared with that of LMWH to antithrombin III in the process of anticoagulation.[27–29]

Inhibitory effect of LHT7 on VEGF$_{165}$-mediated KDR phosphorylation in HUVECs

To determine the mechanism related to the angiostatic properties of LHT7, we studied how it affects the endothelial cell growth. HUVECs were incubated with drugs (LHT7 and LMWH), followed by treatment with $VEGF_{165}$ or with the coincubated mixture of bevacizumab plus $VEGF_{165}$. $VEGF_{165}$ induced the increased cell proliferation. On the other hand, the incubation with LHT7 almost completely blocked the VEGF-induced phosphorylation of VEGFR-2 with similar manner of bevacizumab (Fig. 3*b*). Both binding affinity of LHT7 to $VEGF_{165}$ and $VEGF_{165}$-mediated KDR phosphorylation results show that LHT7 binds to $VEGF_{165}$ and hinders the interactions between $VEGF_{165}$ and VEGFR-2, and ultimately inhibits VEGF receptor-2 phosphorylation, which may affect endothelial cell survival, proliferation, angiogenesis and tumor development.

Antiangiogenic effect of LHT7 in vivo *Matrigel plug assay*

In vivo Matrigel plug assay was carried out to determine whether LHT7 inhibits the angiogenesis induced by $VEGF_{165}$ (Fig. 4). After 10 days of subcutaneous injection into the flank of C3H/HeN mice with 4 different kinds of Matrigel solutions, including positive and negative control groups, LMWH/$VEGF_{165}$ and LHT7/$VEGF_{165}$ groups, Matrigel plugs were removed from mice and their external appearances were photographed (Fig. 4*a*). The positive controlled plugs treated with only $VEGF_{165}$ were dark-brown in color, and the plugs treated with heparin and $VEGF_{165}$ were yellow brown in color, representing the formation of new blood vessels and existing red blood cells within the vessels. On the other hand, the plugs treated with LHT7 and $VEGF_{165}$ were pale in their color like a case of PBS treating negative control group. It indicates that LHT7 was the main cause of a significant decrease in blood vessel formation. The robust blood vessels were visualized in the positive control and LMWH/$VEGF_{165}$ groups by H&E and anti-vWF immunohistochemistry; however, there were few blood vessels and red blood cells in the LHT7/$VEGF_{165}$ groups (Figs. 4*b* and 4*c*). Furthermore, the quantitative

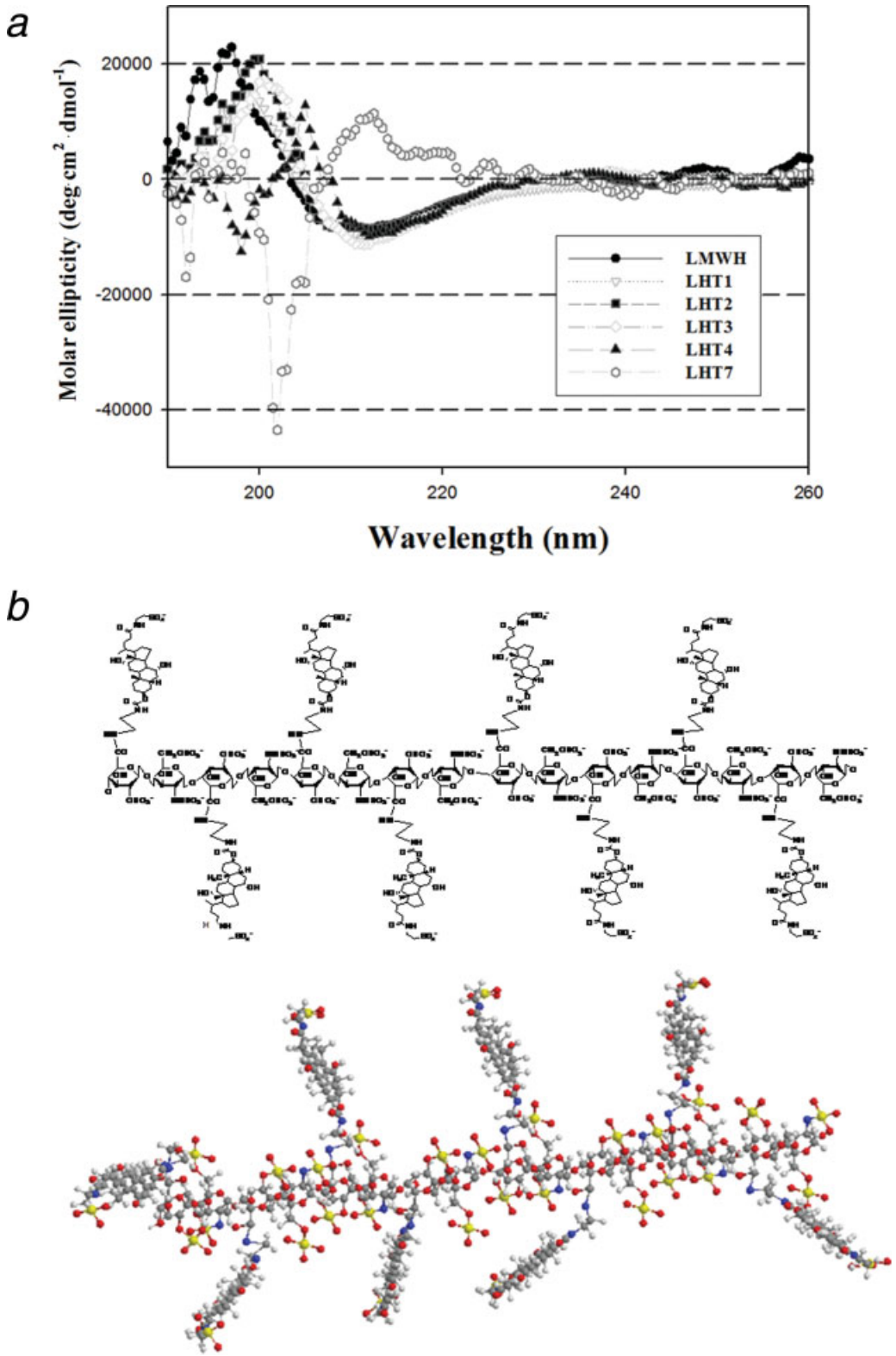

FIGURE 2 – Structural characterization of LHT. (*a*) CD spectra of LHT series. LHT7 showed polyproline-type helical structure compared with other LHT derivatives. (*b*) Chemical structure of LHT7.

analysis of blood formation was performed by determining hemoglobin contents in the Matrigels by using Drabkin's reagent (Fig. 4*d*). LHT7/$VEGF_{165}$ containing Matrigel plugs had 78% less of the hemoglobin amount than the positive control group. These results imply that LHT7 inhibits $VEGF_{165}$-induced angiogenesis *in vivo*.

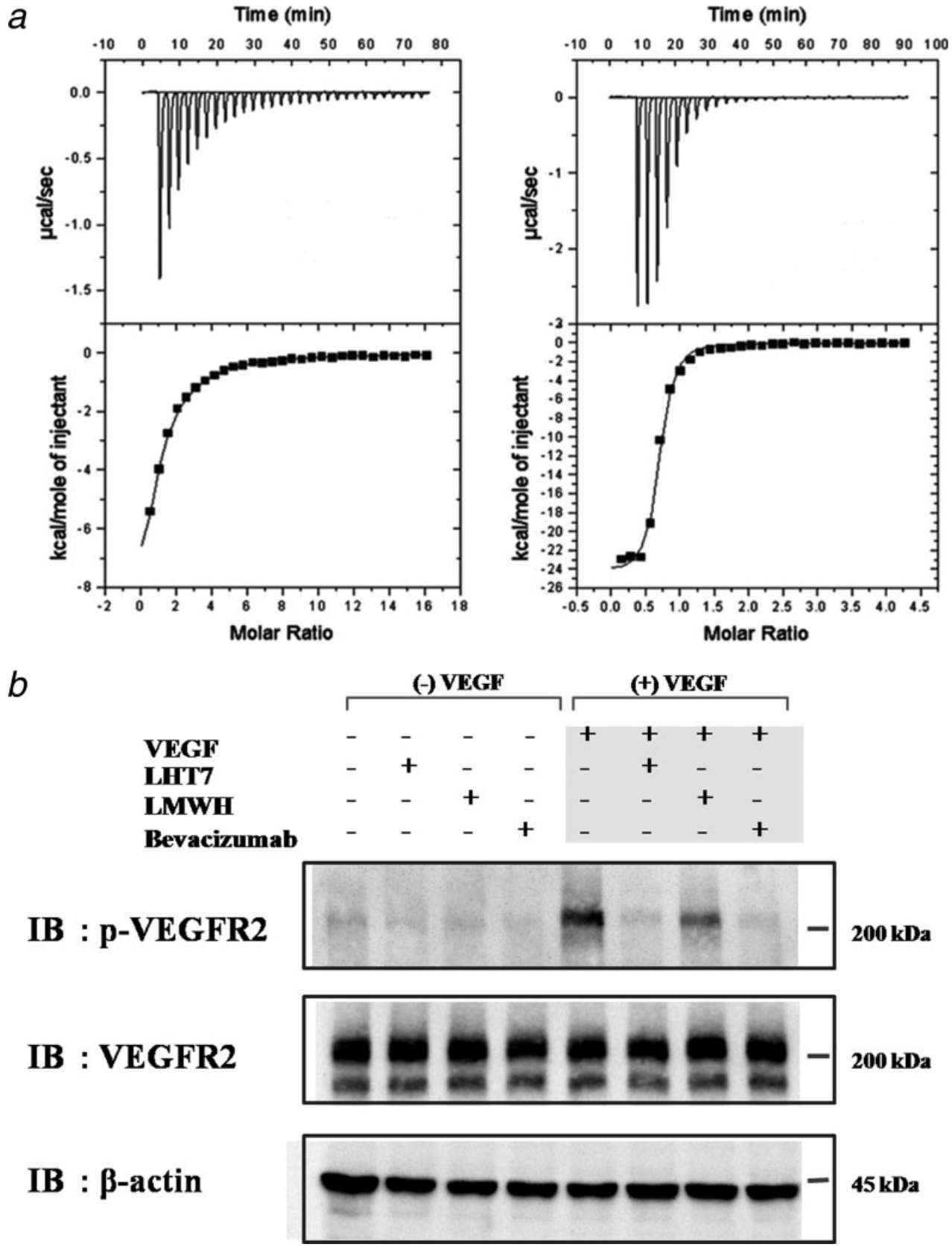

FIGURE 3 – Binding affinity between $VEGF_{165}$ and LMWH or LHT7 and their biological influence in the angiogenesis signal transduction. (*a*) Isothermal titration calorimetry. Dissociation constant (K_d) in making complexes between $VEGF_{165}$ and LMWH (left) or $VEGF_{165}$ and LHT7 (right) were evaluated. (*b*) $VEGF_{165}$ dependent KDR phosphorylation. HUVECs were incubated with 500 ng/ml of LHT7 or the same amount of bevacizumab for 1 hr, followed by treatment with $VEGF_{165}$ (50 ng/ml) for 5 min. Proteins were separated by SDS-PAGE, and the phosphorylated proteins were probed with antiphospho-VEGFR2. β-actin was used as a loading control.

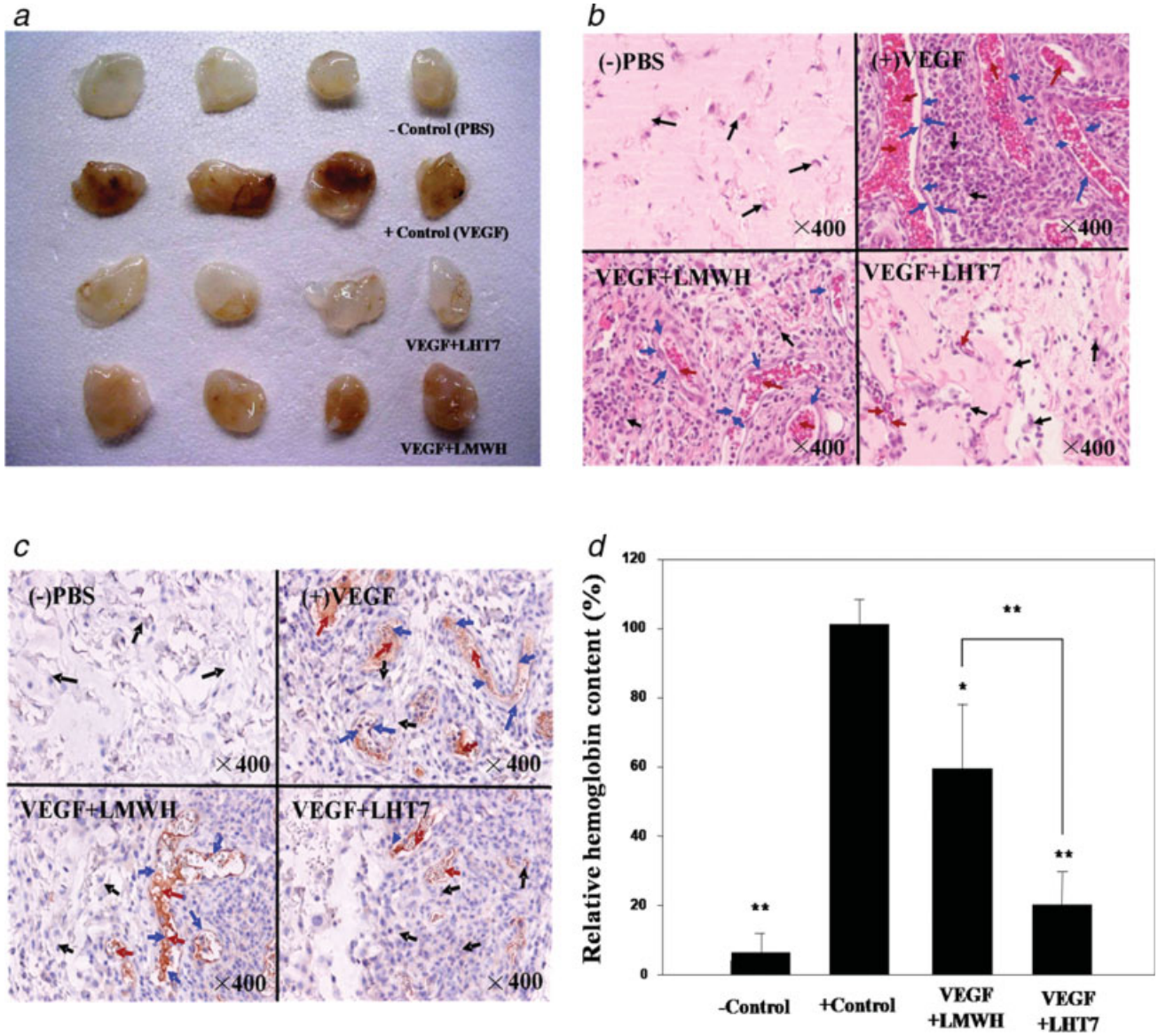

Figure 4 – Inhibition of the VEGF-driven angiogenesis in Matrigel plugs by LHT7. (*a*) Matrigel containing PBS alone (−control), VEGF alone (+control), VEGF+LHT7 and VEGF+LMWH groups were photographed. (*b*) Sections of H&E stained Matrigel plugs were examined by microscopy. Red, blue and black arrows, respectively, indicate red blood cells, blood vessel wall and the background of Matrigel. (*c*) Sections of anti-vWF monoclonal antibody stained Matrigel plugs were examined by microscopy. Red, blue and black arrows, respectively, indicate red blood cells, blood vessel wall and the background of Matrigel. (*d*) Hemoglobin contents within Matrigel plugs were determined by the Drabkin's method. *, $p < 0.005$ *versus* positive control (VEGF alone), **, $p < 0.001$ *versus* positive control (VEGF alone) and **, $p < 0.001$ (LHT7 *versus* LMWH). The error bar represents SE.

Antitumoral effect of LHT in mice

Anticancer effect of LHT was investigated in an *in vivo* tumor graft model using SCC7 cells. SCC7 cells were subcutaneously injected into the flanks of C3H/HeN mice, and subsequent tumor growth and neovascularization were monitored for 15 days after intravenously administering 5 mg/kg/3 day of LMWH, LHT2 and LHT7. LHT7 showed therapeutic potentials in SCC7 cancer disease models. In the first experiment, the LHT7 treated group inhibited tumor growth by 69% compared with the saline treated control group (Fig. 5*a*). However, LHT2, whose anticoagulant activity is about 80%, showed less tumor inhibition effect than LHT7. When LHT7 was treated at 0.5, 1 and 5 mg/kg/day, tumor growth rate was significantly lowered by 63 and 70% in the 1 mg/kg/day and 5 mg/kg/day group compared with the control group (Fig. 5*b*). When LHT7 was administered at the same dosage of 1 mg/kg at different intervals of a day, once/2 days, once/3 days and once a week, it was noted that tumor growth was inhibited dramatically when once per 2 days as well as everyday administrations are given (Fig. 5*c*). Therefore, based on this experiment, 1 mg/kg/2 days of LHT7 was determined as the proper dosage in the mouse model. The survival rates of mice which were treated with saline (control), LMWH and LHT7 were evaluated for about 2 months. On day 35, the survival rates of control, LMWH and LHT7 groups were 25, 50 and 75%, respectively. All the mice with saline treatment died after 46 days of the administration, yet the LMWH and LHT7 groups showed survival rates of 25 and 62.5%, respectively. Moreover, the LHT7 group showed a prolonged survival rate above 60% for about 70 days (Fig. 5*d*).

The antitumor effect of LHT7 in mice was evaluated using MDA-MB231 human breast carcinoma. When the mice were

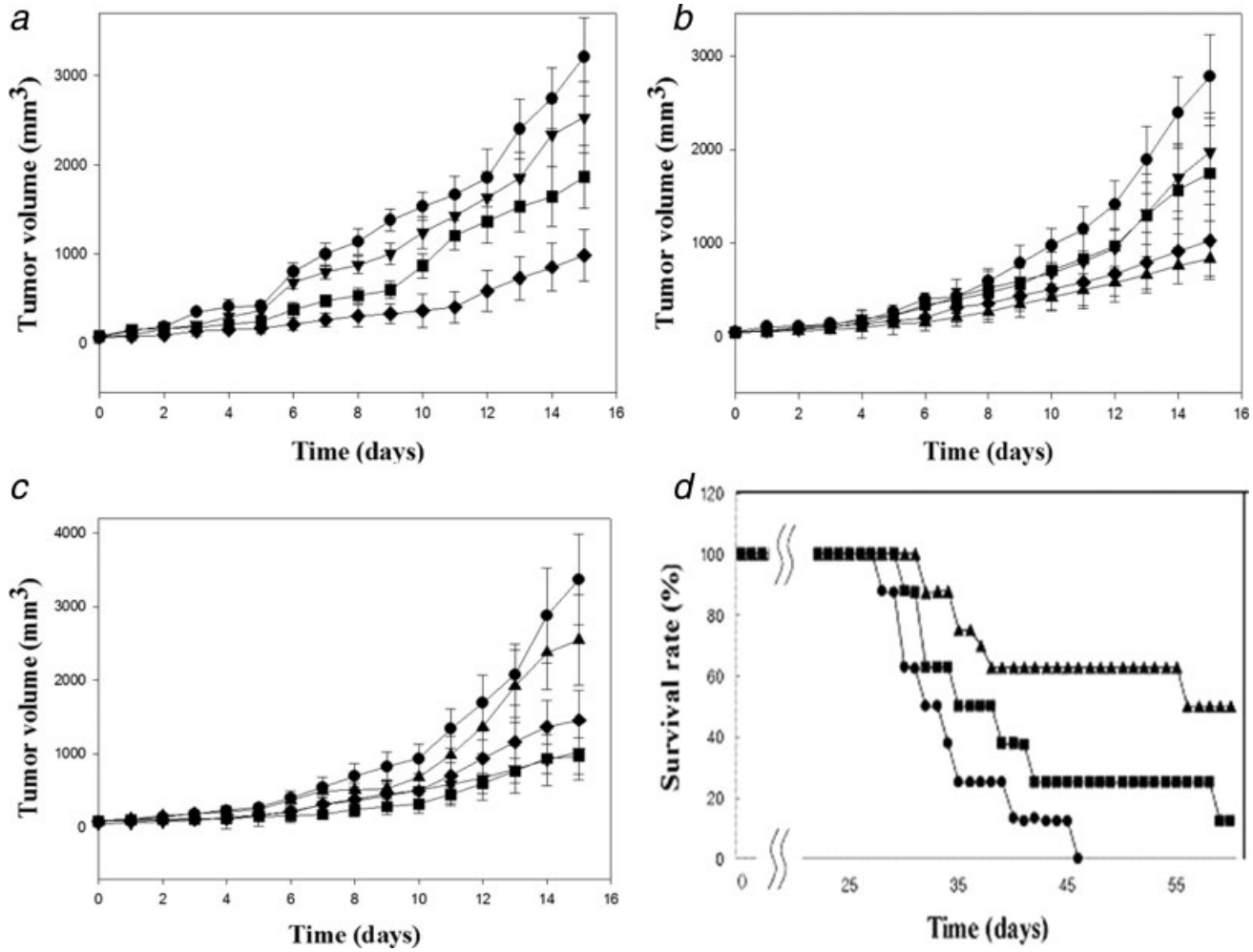

Figure 5 – Antitumoral effect of LHT7 on SCC7 grafted mice. (*a*) Tumor growth curves for saline (● control), LMWH (▼ 5 mg/kg/3 day), LHT2 (■ 5 mg/kg/3 day) and LHT7 (♦ 5 mg/kg/3 day). (*b*) Tumor growth curves for saline (● control), LMWH (▼ 5 mg/kg/day), LHT7 (■ ; 0.5 mg/kg/day, ♦; 1 mg/kg/day, ▲; 5 mg/kg/day). (*c*) Tumor growth curves for saline (● control), LHT7 1 mg/kg (▼; daily, ■; once/2 day, ♦; once/3 day and ▲; once/week). Each group contained 8 or 9 to mice and the sizes of tumors were measured daily. (*d*) Survival rate. LHT7 (▲1 mg/kg/2 day), LMWH (■ 5 mg/kg/2 day, Saline (● Control).

treated with LHT7, the tumor growth rates were much slower than the control group. LHT7 at 1 and 5 mg/kg/day significantly decreased tumor volumes by 85.6% and 90.3%, respectively. The *in vivo* antiangiogenic or antiproliferating activity of LHT7 in the MDA-MB231 human breast cancer xenograft model was confirmed using the CD34 and Ki67 immunohistochemistry staining assay. Treatments with LHT7 of 1 mg/kg/day and LHT of 5 mg/kg/day decreased the number of CD34 positive blood vessels by 74.3% and 85.1%, respectively, compared with the control group. Moreover, LHT7 at 1 and 5 mg/kg/day inhibited the cell proliferation by 56.6% and 70.4%, compared with the control group (Fig. 6).

Discussion

The angiogenesis phenomenon of new blood vessel formation has been considered as a crucial process in tumor development, because tumor cells maintain their continuous growth by obtaining sufficient oxygen and nutrients from blood vessels. In terms of angiogenesis, we can consider diverse factors such as bFGF, VEGF, PDGF, heparanase and several MMPs. Although there are many kinds of angiogenesis promoters, one of the most important factors is vascular endothelial growth factor (VEGF). Among several VEGF isoforms including $VEGF_{121}$, $VEGF_{165}$, $VEGF_{189}$ and $VEGF_{206}$, $VEGF_{165}$ is a major form which promotes angiogenesis significantly.[29] This study shows that the polyproline-type helical structured LHT7 could inhibit $VEGF_{165}$ dependent angiogenesis and further developments of tumors by restricting nutrient supply. Also this study reveals that LHT7 has specialized physical and structural properties to block $VEGF_{165}$-dependent angiogenesis successfully compared with LMWH.

The polyproline-type helical structured LHT7 could efficiently prevent tumor development *in vivo* by restricting angiogenesis. In the case of intravenous treatments with LHT7, tumor growth was significantly inhibited compared with the control group in both SCC7 murine cancer cell and MDA-MB231 human breast carcinoma. The development of a tumor size is directly related to the formation of new blood vessels in the tumor tissues. According to the histological results of MDA-MB231 tumor tissues, we could show LHT7 inhibited angiogenesis and further cell proliferation effectively. By preventing tumor tissues from making new blood vessels through LHT7 treatment, we showed that tumor growth was dramatically delayed. In this study, we showed that LHT7 could inhibit the angiogenesis in MDA-MB231 human breast carcinoma, and its angiogenesis inhibitory effect was clearly shown by the $VEGF_{165}$-dependent *in vivo* Matrigel plug assay. In this

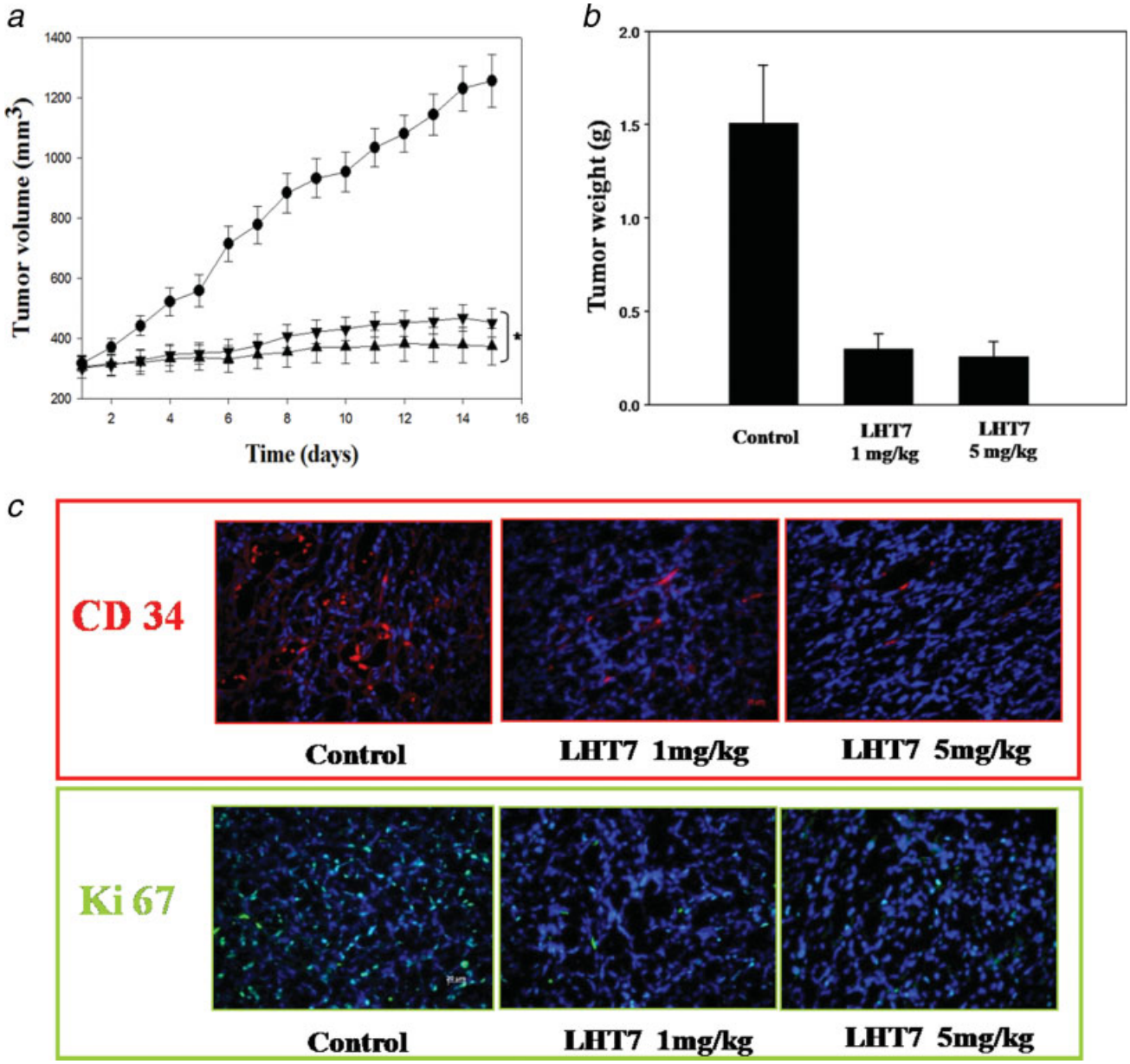

FIGURE 6 – MDA-MB 231 tumor growth inhibition. (*a*) Tumor growth curves for saline (♦ control), LHT7 (■; 1 mg/kg/day, ●; 5 mg/kg/day). *, $p < 0.0001$ *versus* control. (*b*) Tumor weight. The error bar represents SE ($n = 8$ or 9). *, $p < 0.001$ *versus* control. The inset p value in figure indicated the significances between groups. (*c*) Immunohistochemistry with CD34, Ki67 of experimental tumor tissue. The administration of LHT7 (1, 5 mg/kg/day) decreased the number of CD34 positive blood vessels 74.3% and 85.1%, respectively, compared with the control group. LHT7 at (1, 5 mg/kg/day) also inhibited the cell proliferation by 56.6% and 70.4% compared with the case of control group.

assay, LHT7/$VEGF_{165}$ group had much lower amount of hemoglobin than the positive control group. Moreover, in the HUVECs tubular formation experiment, LHT7 dramatically inhibited the organization of endothelial cells into the tubular structure more significantly compared with the case of control and LMWH groups (data not shown).

To clearly confirm the action mechanism of LHT7, we carried out $VEGF_{165}$-mediated KDR phosphorylation assay. In this assay, we showed that LHT7 blocked the phosphorylation of $VEGF_{165}$ receptor as bevacizumab, the monoclonal antibody of $VEGF_{165}$ did. In this regard, LHT7 played a crucial role as an angiogenesis inhibitor by interfering with the interaction between $VEGF_{165}$ and its receptors. To learn how LHT7 physically neutralize $VEGF_{165}$ activity, the binding affinity between $VEGF_{165}$ and LHT7 was determined by using isothermal titration calorimetry in a solution state. In this experiment, we showed that LHT7 could bind to $VEGF_{165}$ with a dissociation constant of $(3.21 \pm 0.04) \times 10^{-7}$ M, which means that LHT7 binds to $VEGF_{165}$ better than LMWH does, with ~60 times stronger affinity. In particular, the 10^{-7} ordered dissociation constant in the binding of LHT7 to $VEGF_{165}$ is comparable to the binding affinity between antithrombin III and LMWH in a biological coagulation process.[30] This explains how the binding affinity between LHT7 and $VEGF_{165}$ is strong enough to be sustained in the biological environment as well as *in vitro* condition, as antithrombin III can readily interact with LMWH in a human body.

It has been reported that $VEGF_{165}$ has its own heparin binding domain (HBD) which represents residues from 111 to 165. In this

domain, there are a number of basic amino acids such as Arg 124, 145, 156, 159 and Lys 140. The HBD mainly interacts with the sulfate and carboxylic acid groups of LMWH.[31] Based on this fact, LMWH has been studied as an active compound which can inhibit VEGF functions; it has also been proposed as a potent anticancer agent. However, the therapeutic effect of LMWH is so trivial that it cannot be applied clinically and the repetitive administration of LMWH can result in a considerable side effect of bleeding. On the other hand, LHT7 overcame these drawbacks of LMWH, since LHT7 has much better potency in cancer treatments and a minimized anticoagulant activity that is ~12% level of LMWH by completely conjugating taurocholate moieties on LMWH.

The significant improvement in the antiangiogenic activity of LHT7 over LMWH can be explained by the following. LHT7 has more sulfate groups than LMWH due to its taurocholate moieties which have negatively charged sulfate groups. Although all of the carboxylic acid groups were occupied for chemical conjugation with taurocholate moieties, additional sulfate groups can compensate for their total charge condition. The considerable degree of sulfation is favorable to the binding of growth factors to their receptors, which have positive charged amino acid residues. We confirmed that LHT7 has a polyproline-type helical structure using the circular dichroism spectra, which showed that the structure of LHT7 is different from other LHT derivatives. LHT7 has 7 or 8 numbers of bulky taurocholate moieties with relatively constant distances on the flexible hydrophilic LMWH, thus forming a helical structure as well as a rigid formation compared with the random structure of LMWH and other unsaturated LHTs. In addition, hydrophobic cholesteryl ring structure of taurocholate moiety can contribute to the hydrophobic interaction between LHT7 and $VEGF_{165}$.

VEGF targeted therapies has been proposed owing to the fundamental roles of VEGF in angiogenesis and further tumorigenesis. Some VEGF antagonists or VEGF receptor inhibitors have been discovered at present.[32–34] However, these inhibitors have various drawbacks such as high drug resistance, severe toxicities and great expense to generate.[35,36] LHT7 may have potential value as a therapeutic agent to prevent angiogenesis and delay tumor development. It can be used conveniently and safely, since heparin is a nontoxic biomolecule. Even though heparin has a drawback of hemorrhage, the anticoagulant activity of LHT7 is just at 12% level of LMWH, so its usage in therapeutic dosages has no problem. Also, the survival rates of mice in tumor inhibition experiments showed a promising level of anticancer activity for LHT7. LHT7 group showed a prolonged survival rate above 60% for about 60 days while maintaining their normal body weight. This explains that LHT7 showed tumor inhibition ability without severe toxicity.

In summary, our study showed that the polyproline-type helical structured LHT7 could have significant antiangiogenic effects by blocking interaction between $VEGF_{165}$ and its receptors by strongly binding to $VEGF_{165}$, thus deterring angiogenesis signals through $VEGF_{165}$ receptors. Owing to its angiogenesis inhibitory effect, LHT7 can also delay tumor growth significantly in both SCC7 murine cancer cell line and MDA-MB231 human breast carcinoma. Based on these findings, LHT7 could be a more suitable candidate for coadministration with other anticancer drugs without certain drawbacks, or for the first line of cancer therapy, because LHT7 has a dramatic therapeutic potential with lower side effects.

References

1. Folkman J. Tumor angiogenesis: therapeutic implications. N Engl J Med 1971;285:1182–6.
2. Brem S, Brem H, Folkman J, Finkelstein D, Patz A. Prolonged tumor dormancy by prevention of neovascularization in the vitreous. Cancer Res 1976;36:2807–12.
3. Parangi S, Dietrich W, Christofori G, Lander ES, Hanahan D. Tumor suppressor loci on mouse chromosomes 9 and 16 are lost at distinct stages of tumorigenesis in a transgenic model of islet cell carcinoma. Cancer Res 1995;55:6071–6.
4. Griffioen AW, Molema G. Angiogenesis: potentials for pharmacologic intervention in the treatment of cancer, cardiovascular diseases and chronic inflammation. Pharmacol Rev 2000;52:237–68.
5. Carmeliet P, Jain RK. Angiogenesis in cancer and other diseases. Nature 2000;407:249–57.
6. Senger DR, Perruzzi CA, Feder J, Dvorak HF. A highly conserved vascular permeability factor secreted by a variety of human and rodent tumor cell lines. Cancer Res 1986;46:5629–32.
7. Schmidt NO, Westphal M, Hagel C, Ergun S, Stavrou D, Rosen EM, Lamszus K. Levels of vascular endothelial growth factor, hepatocyte growth factor/scatter factor and basic fibroblast growth factor in human gliomas and their relation to angiogenesis. Int J Cancer 1999; 84:10–18.
8. Kumar R, Kuniyasu H, Bucana CD, Wilson MR, Fidler IJ. Spatial and temporal expression of angiogenic molecules during tumor growth and progression. Oncol Res 1998;10:301–11.
9. Smorenburg SM, Van Noorden CJ. The complex effects on heparins on cancer progression and metastasis in experimental studies. Pharmacol Rev 2001;53:93–105.
10. Folkman J, Langer R, Linhardt RJ, Haudenschild C, Taylor S. Angiogenesis inhibition and tumor regression caused by heparin or a heparin fragment in the presence of cortisone. Science 1983;221:719–25.
11. Schlessinger J, Lax I, Lemmon M. Regulation of growth factor activation by proteoglycans: what is the role of the low affinity receptors? Cell 1995;83:357–60.
12. Soker S, Goldstaub D, Svahn CM, Vlodavsky I, Levi BZ, Neufeld G. Variations in the size and sulfation of heparin modulate the effect of heparin on the binding of VEGF165 to its receptors. Biochem Biophys Res Commun 1994;203:1339–47.
13. Tessler S, Rockwell P, Hicklin D, Cohen T, Levi BZ, Witte L, Lemischka IR, Neufeld G. Heparin modulates the interaction of VEGF165 with soluble and cell associated flk-1 receptors. J Biol Chem 1994;269:12456–61.
14. Jayson GC, Gallagher JT. Heparin oligosaccharides: inhibitors of the biological activity of bFGF on Caco-2 cells. Br J Cancer 1997;75:9–16.
15. Hirsh J. Heparin. N Engl J Med 1991;324:1565–74.
16. Jaques LB. Heparins: anionic polyelectrolyte drugs. Pharmacol Rev 1979;31:99–166.
17. Jin L, Abrahams JP, Skinner R, Petitou M, Pike RN, Carrell RW. The anticoagulant activation of antithrombin by heparin. Proc Natl Acad Sci USA 1997;94:14683–8.
18. Hettiarachchi RJ, Smorenburg SM, Ginsberg J, Levine M, Prins MH, Buller HR. Do heparins do more than just treat thrombosis? The influence of heparins on cancer spread. Thromb Haemostasis 1999;82: 947–52.
19. Thorpe PE, Derbyshire EJ, Andrade SP, Press N, Knowles PP, King S, Watson GJ, Yang YC, Rao-Bette M. Heparin-steroid conjugates: new angiogenesis inhibitors with antitumor activity in mice. Cancer Res 1993;53:3000–7.
20. Park K, Lee GY, Kim YS, Yu M, Park RW, Kim IS, Kim SY, Byun Y. Heparin-deoxycholic acid chemical conjugate as an anticancer drug carrier and its antitumor activity. J Control Release 2006;114: 300–6.
21. Park K, Kim YS, Lee GY, Nam JO, Lee SK, Park RW, Kim SY, Kim IS, Byun Y. Antiangiogenic effect of bile acid acylated heparin derivative. Pharm Res 2007;24:176–85.
22. Yu MK, Lee DY, Kim YS, Park K, Park SA, Son DH, Lee GY, Nam JH, Kim SY, Kim IS, Park RW, Byun Y. Antiangiogenic and apoptotic properties of a novel amphiphilic folate-heparin-lithocholate derivative having cellular internality for cancer therapy. Pharm Res 2007; 24:705–14.
23. Pumphrey CY, Theus AM, Li S, Parrish RS, Sanderson RD. Neoglycans, carbodiimide-modified glycosaminoglycans: a new class of anticancer agents that inhibit cancer cell proliferation and induce apoptosis. Cancer Res 2002;62:3722–8.
24. Eriksson S, Sjovall J. The absorption spectra of bile acids in sulfuric acid. Ark Kemi 1955;8:303–11.
25. Nichifor M. Carpov A. Bile acids covalently bound to polysaccharides. I. Ester of bile acids with dextran. Eur Polym J 1999;35:2125–9.
26. Nichifor M, Stanciu MC, Zhu XX. Bile acids covalently bound to polysaccharides. II. Dextran with pendant cholic acid groups. React Funct Polym 2004;59:141–8.
27. Rabanal F, Ludevid MD, Pons M, Giralt E. CD of proline-rich polypeptides: application to the study of the repetitive domain of maize glutelin-2. Biopolymers 1993;33:1019–28.

28. Ma K, Kan L, Wang K. Polyproline II helix is a key structural motif of the elastic PEVK segment of titin. Biochemistry 2001;40:3427–38.
29. Ferrara N, Gerber HP, LeCouter J. The biology of VEGF and its receptors. Nat Med 2003;9:669–76.
30. Cross RT, Sobel M, Marques D, Harris RB. Heparin binding domain peptides of antithrombin III: analysis by isothermal titration calorimetry and circular dichroism spectroscopy. Protein Sci 1994;3: 620–7.
31. Robinson CJ, Mulloy B, Gallagher JT, Stringer SE. VEGF165-binding sites within heparan sulfate encompass two highly sulfated domains and can be liberated by K5 lyase. J Biol Chem 2006; 281:1731–40.
32. Presta LG, Chen H, O'Connor SJ, Chisholm V, Meng YG, Krummen L, Winkler M, Ferrara N. Humanization of an anti-vascular endothelial growth factor monoclonal antibody for the therapy of solid tumors and other disorders. Cancer Res 1997;57:4593–9.
33. Mendel DB, Laird AD, Xin X, Louie SG, Christensen JG, Li G, Schreck RE, Abrams TJ, Ngai TJ, Lee LB, Murray LJ, Carver J, et al. In vivo antitumor activity of SU11248, a novel tyrosine kinase inhibitor targeting vascular endothelial growth factor and platelet-derived growth factor receptors: determination of a pharmacokinetic/pharmacodynamic relationship. Clin Cancer Res 2003;9:327–37.
34. Holash J, Davis S, Papadopoulos N, Croll SD, Ho L, Russell M, Boland P, Leidich R, Hylton D, Burova E, Ioffe E, Huang T, et al. VEGF-Trap: a VEGF blocker with potent antitumor effects. Proc Natl Acad Sci USA 2002;99:11393–8.
35. Verheul H, Pinedo HM. Possible molecular mechanisms involved in the toxicity of angiogenesis inhibition. Nat Rev Cancer 2007;7:475–85.
36. Robert C, Faivre S, Raymond E, Armand JP, Escudier B. Subungual splinter hemorrhages: a clinical window to inhibition of vascular endothelial growth factor receptors. Ann Intern Med 2005;143:313–4.